Electronic Supplementary Material (ESI) for Journal of Materials Chemistry A.

Supplemental Information

Defect-engineered MOF-801 for cycloaddition of CO_2 with epoxides

Yunjang Gu, [a] Bai Amutha Anjali, [a] Sunghyun Yoon, [a] Youngson Choe, [a] Yongchul G. Chung,* [a] and Dae-Won Park* [a]

[a]*School of Chemical Engineering, Pusan National University, Busan, 46241, Korea*

*Corresponding author: dwpark@pusan.ac.kr (D.W. Park), drygchung@gmail.com (Y.G. Chung)

List of Table

Table S1 Simulated and experimental BET area computed by SESAMI.

MOF-801	BET area (m^2/g)
Perfect crystal	686
mc-1	966
mc-2	1313
mc-3	1125
mc-4	1322
ml-1	672
ml-2	684
ml-3	696
ml-4	657
ml-5	747
Experimental MOF-801(D)	832
Experimental MOF-801(P)	707

mc: missing cluster, ml: missing linker.

Table S2 Different constraints used for the linear programming.

Method	Constraint
1	- Pressure range - 0 ~ 0.0001 bar
2	- Pressure range - 0 ~ Monolayer coverage pressure point
3	- Pressure range - 0~ Monolayer coverage pressure point - Saturation loading - Relative error of saturation loading between master model isotherm and the experiment should be in plus or minus 5 %
4	- Pressure range - 0~ Monolayer coverage pressure point - Saturation loading - Relative error of saturation loading between master model isotherm and the experiment should be in plus or minus 10 % - Loading at low pressure - Relative error of loading at 0.0001 bar should be in plus or minus 10 %
5	- Pressure range - 0~ Monolayer coverage pressure point - Saturation loading - Relative error of saturation loading between master model isotherm and the experiment should be in plus or minus 10 % - BET-surface area - Relative error of calculated BET-surface area between master model isotherm and the experiment should be in plus or minus 10 %

List of Figures

to form chloropropene carbonate.

Fig. S15 N_2 adsorption isotherms of MOF-801(D) and MOF-801(P).

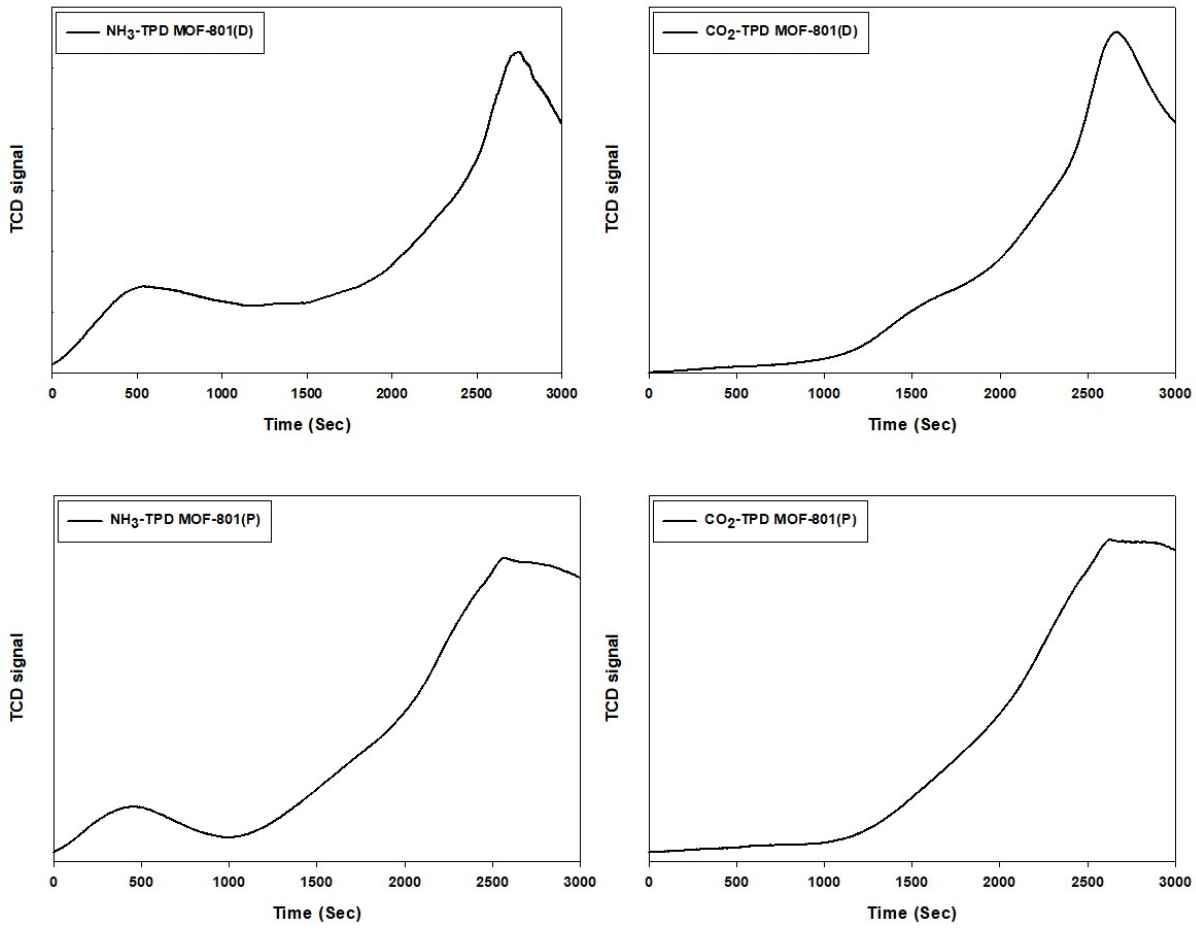

Fig. S1 NH_3 and CO_2-TPD curves of MOF-801(D) and MOF-801(P).

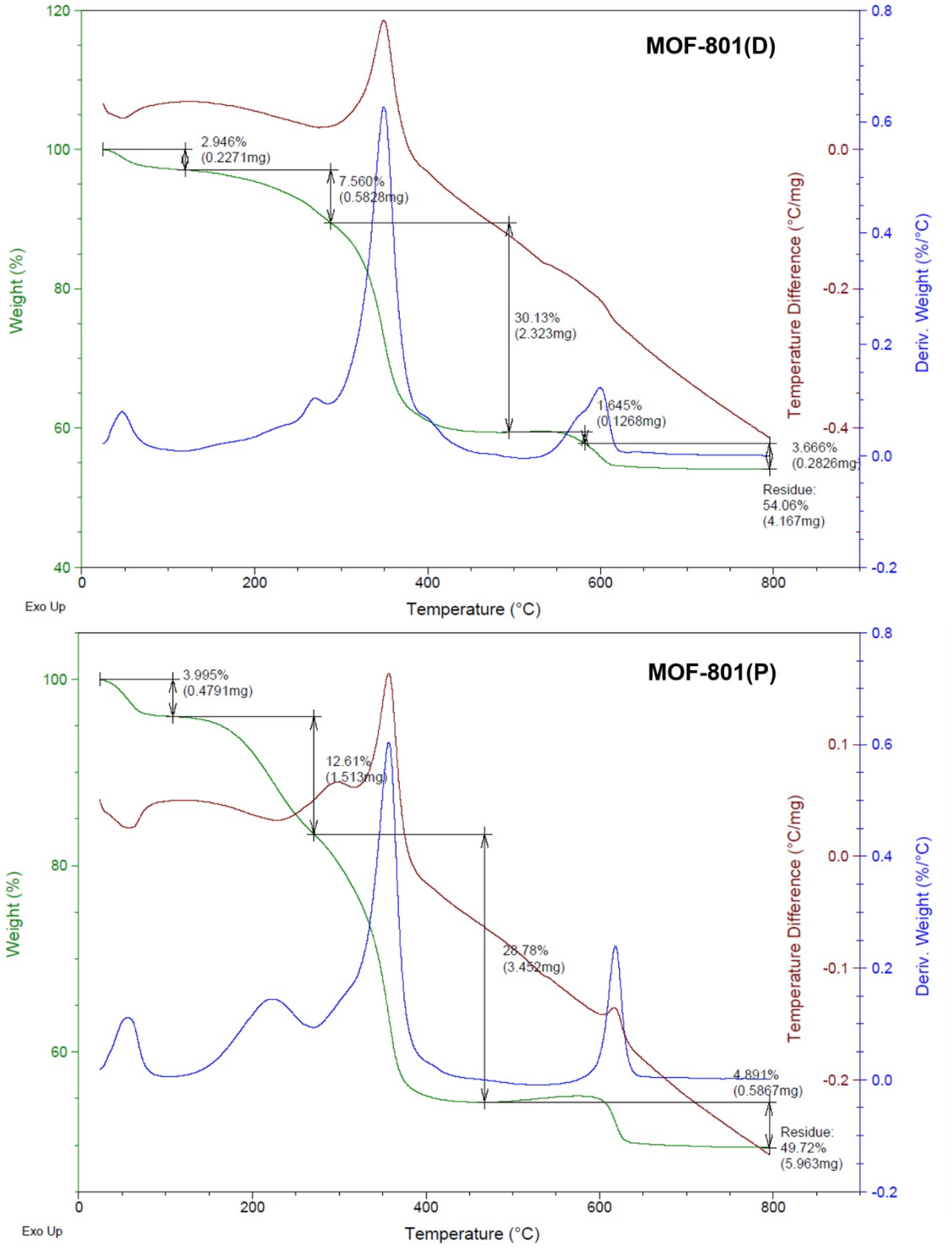

Fig. S2 Thermogravimetric analysis (TGA) and derivative thermogravimetry analysis (DTA) curves of MOF-801(D), and MOF-801(P). Calculation of fumarate ligands in MOF-801.

Calculation of fumarate ligands in MOF-801

MOF-801(P) showed larger weight loss near 400 °C than MOF-801(D). Since MOF-801(P) contains more fumarate ligands in the framework, the weight loss originated from their decomposition could be higher than MOF-801(D) containing smaller number of the ligands. The total weight loss in wt.% between 100 °C (ligand containing state) and 500 °C (ligands are decomposed) for MOF-801(P) and MOF-801(D) was calculated to be 43.1% and 38.8%, respectively. The detailed calculations are;

MOF-801(P): (96.005-54.611)/96.005 = 43.1 %

MOF-801(D): (97.054-59.371)/97.054 = 38.8 %

Since dehydrated formula of MOF-801 is known as $Zr_6O_6(O_2C\text{-}(CH)_2\text{-}CO_2)_6$, theoretical loss of all ligands to be calculated as follows:

MW of $Zr_6O_6(O_2C\text{-}(CH)_2\text{-}CO_2)_6$ = 1327.448

MW of $(ZrO_2)_6$ = 739.272

Theoretical loss of ligands in perfect crystal: (1327.448-739.272)/1327.448 = 44.3 %

One can see that MOF-801(P) is close to the perfect crystal.

If one of six ligands in the formula is missing to form a defect structure,

MW of $Zr_6O_6(O_2C\text{-}(CH)_2\text{-}CO_2)_5$ = 1207.45

Then estimated weight loss will be: (1207.45-739.272)/1207.45 = 38.8 %

Therefore, we can estimate that almost 1/6 ligand of its perfect crystal structure was missed in MOF-801 (D).

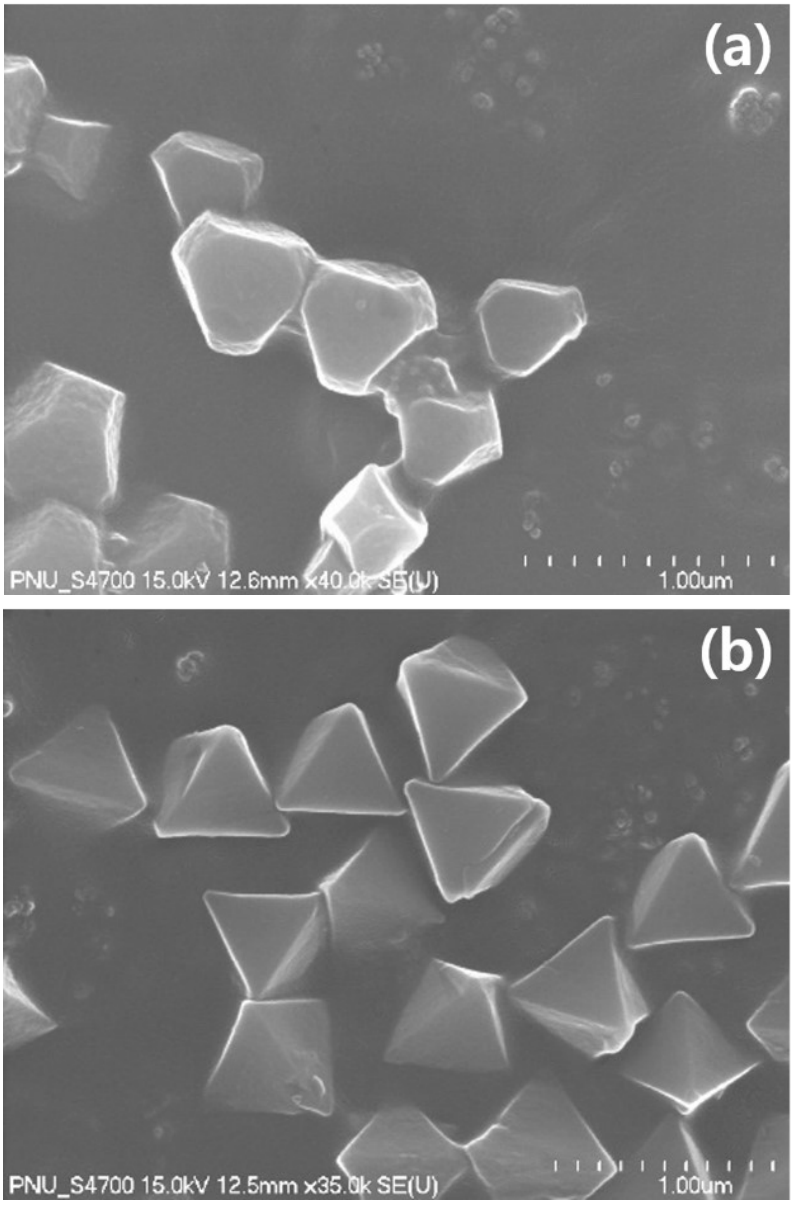

Fig. S3 FE-SEM images of synthesized samples at different condition: (a) MOF-801(D), (b) MOF-801(P).

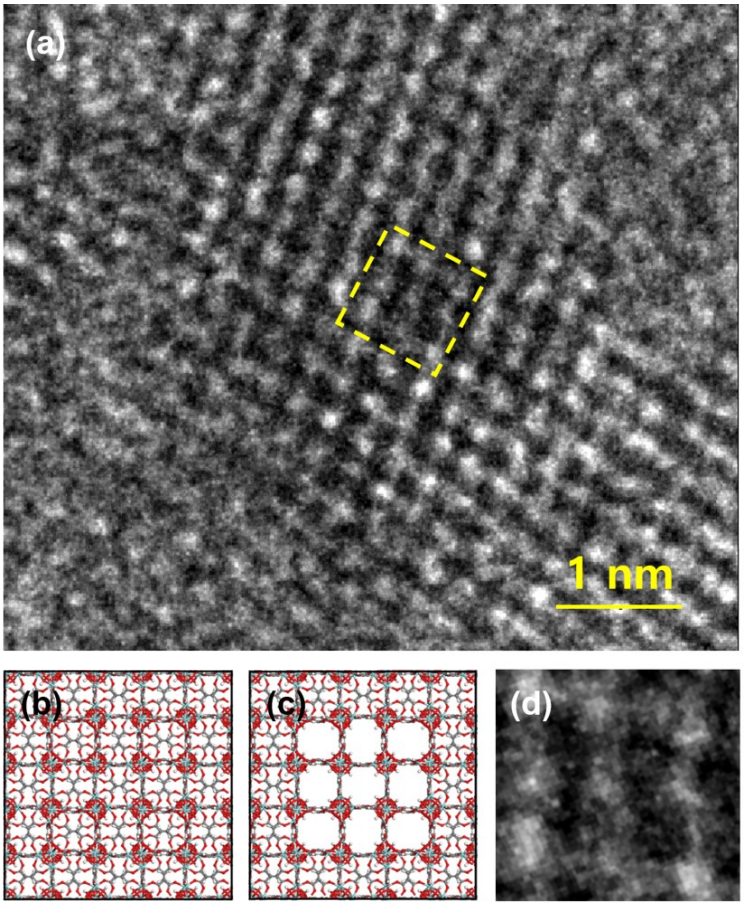

Fig. S4 HR-TEM analysis of the defects in MOF-801(D) (a) HR-TEM image, (b) perfect crystal model, (c) defective structure model, (d) experimental image of defects.

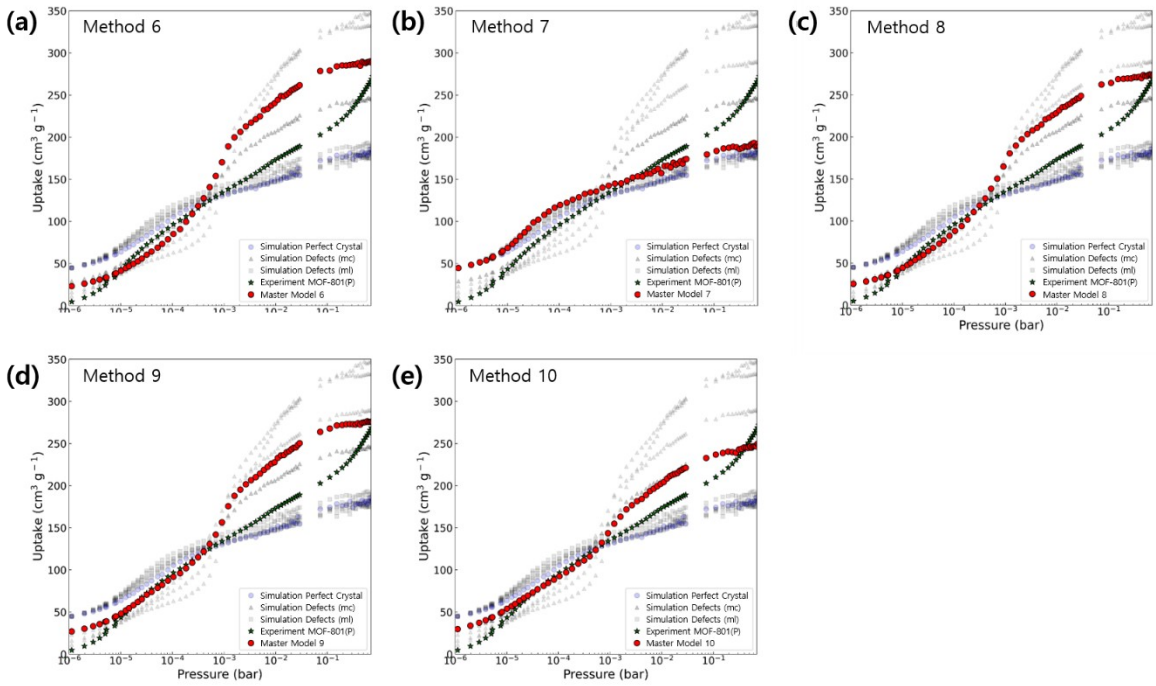

Fig. S5 N_2 master model isotherm of MOF-801(P) at 77 K.

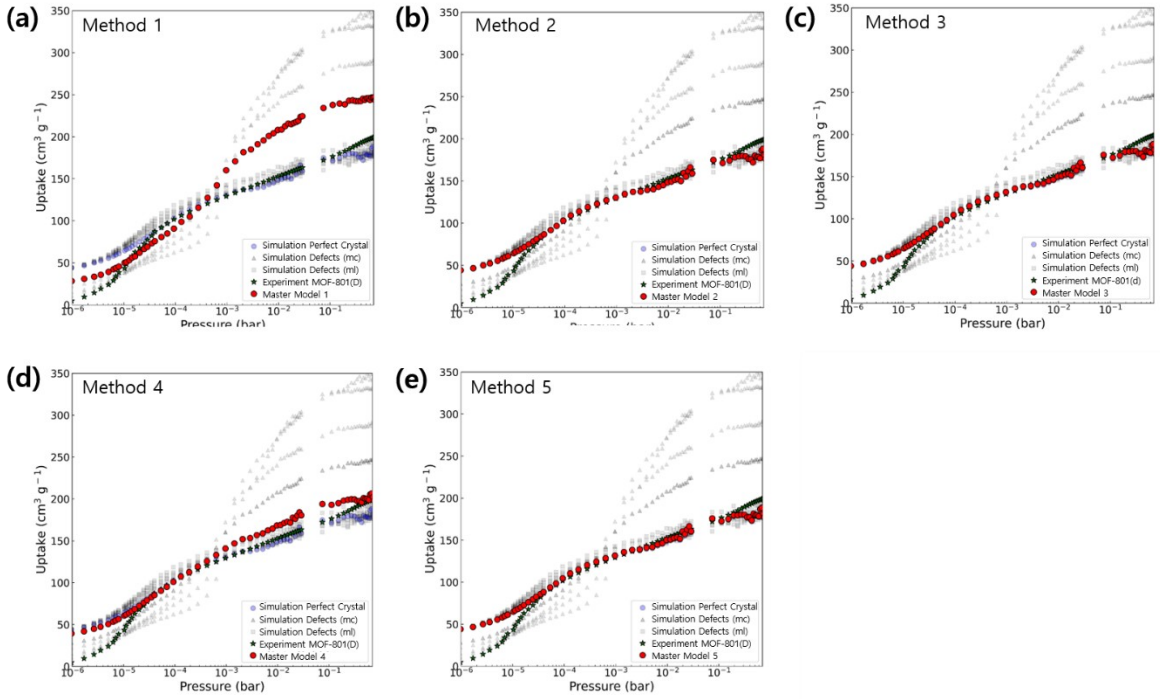

Fig. S6 N_2 master model isotherm of MOF-801(D) at 77 K.

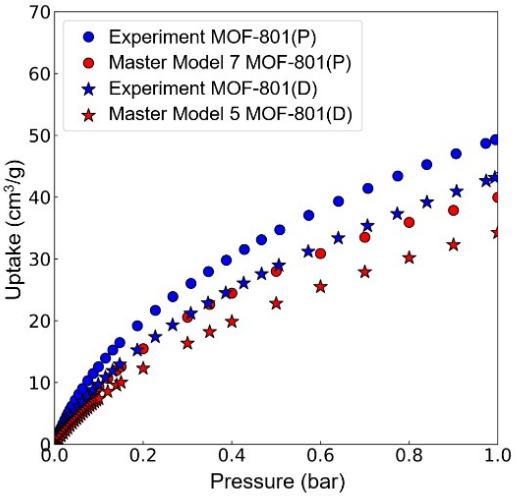

Fig. S7 Comparison of CO_2 adsorption isotherms at 298 K for MOF-801(D) and MOF-801(P) with master isotherm.

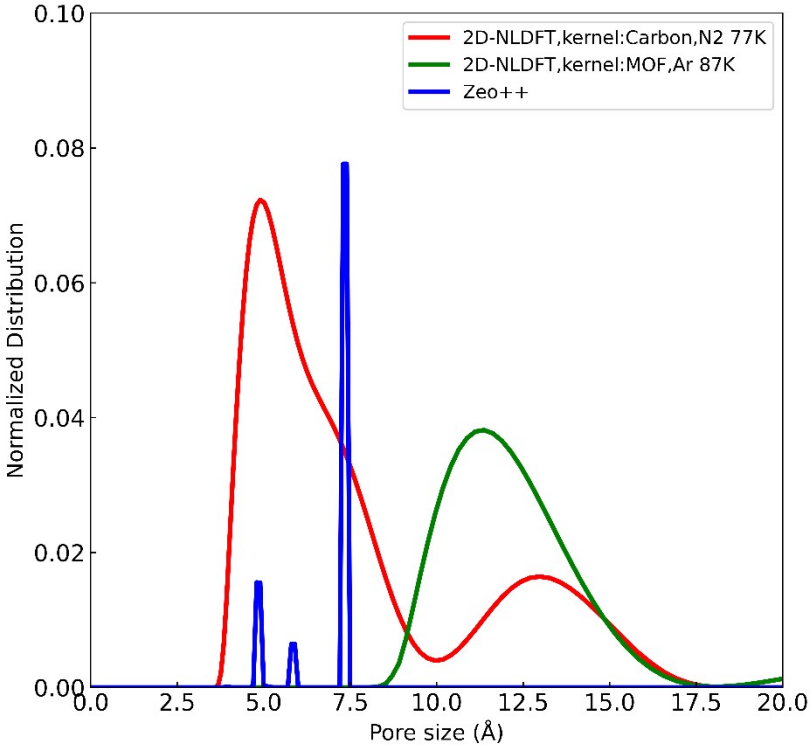

Fig. S8 Comparison between two methods 2D-NLDFT and Zeo++ PSD result for the kernel selection.

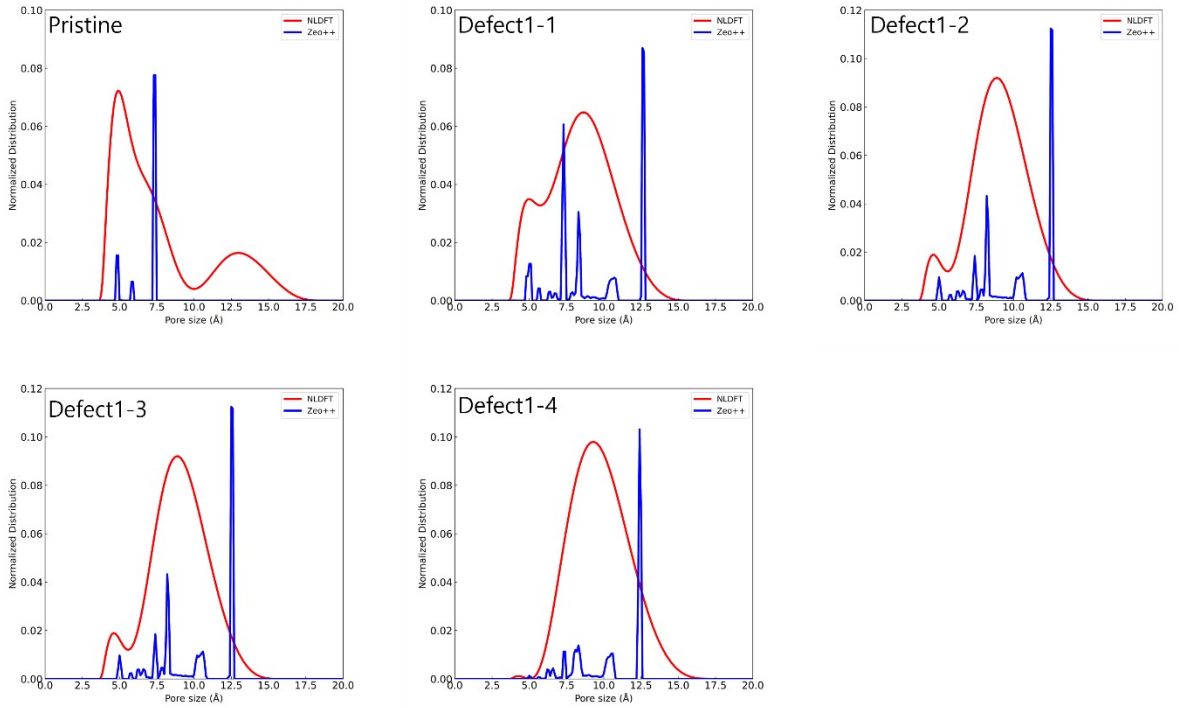

Fig. S9 Comparison between 2D-NLDFT (Carbon, 77 K, N_2 kernel) and Zeo++ PSD for pristine and Defect 1-1 to Defect 1-4.

Fig. S10 Comparison between 2D-NLDFT (Carbon, 77 K, N_2 kernel) and Zeo++ PSD for pristine and Defect 2-1 to Defect 2-5.

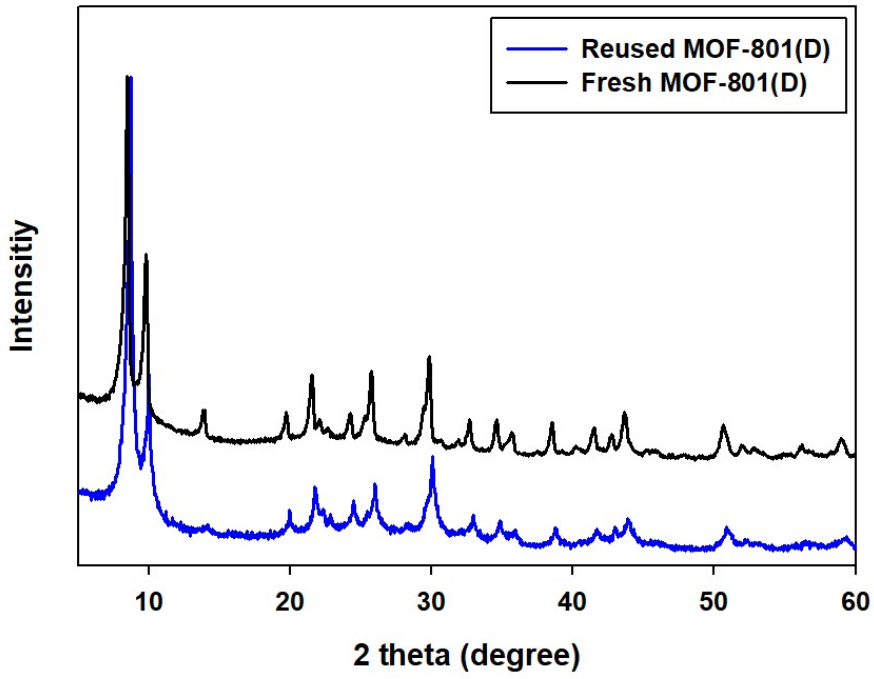

Fig. S11 PXRD patterns of reused MOF-801(D) catalyst.

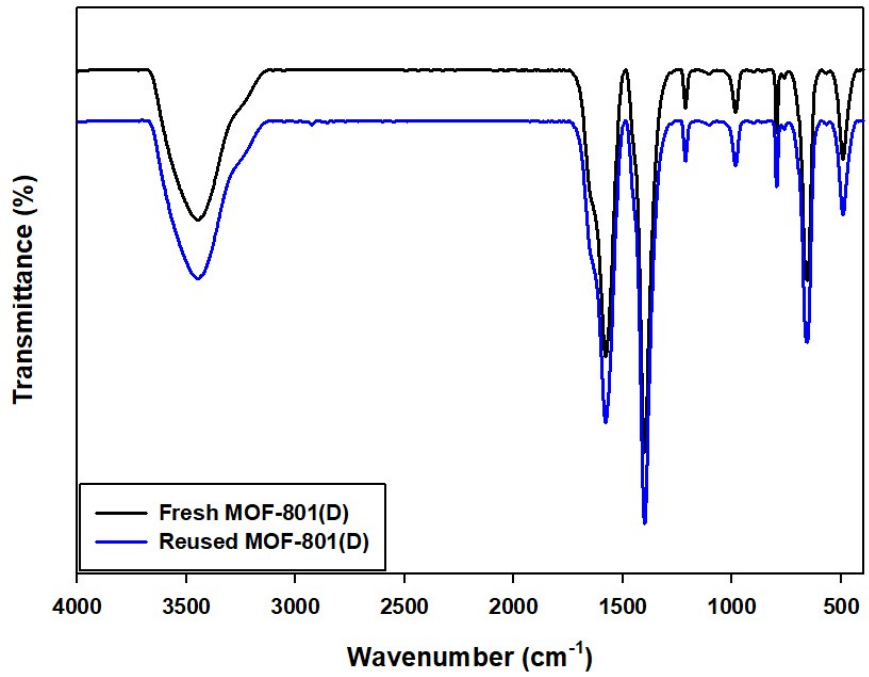

Fig. S12 FT-IR spectra of reused MOF-801(D) catalyst.

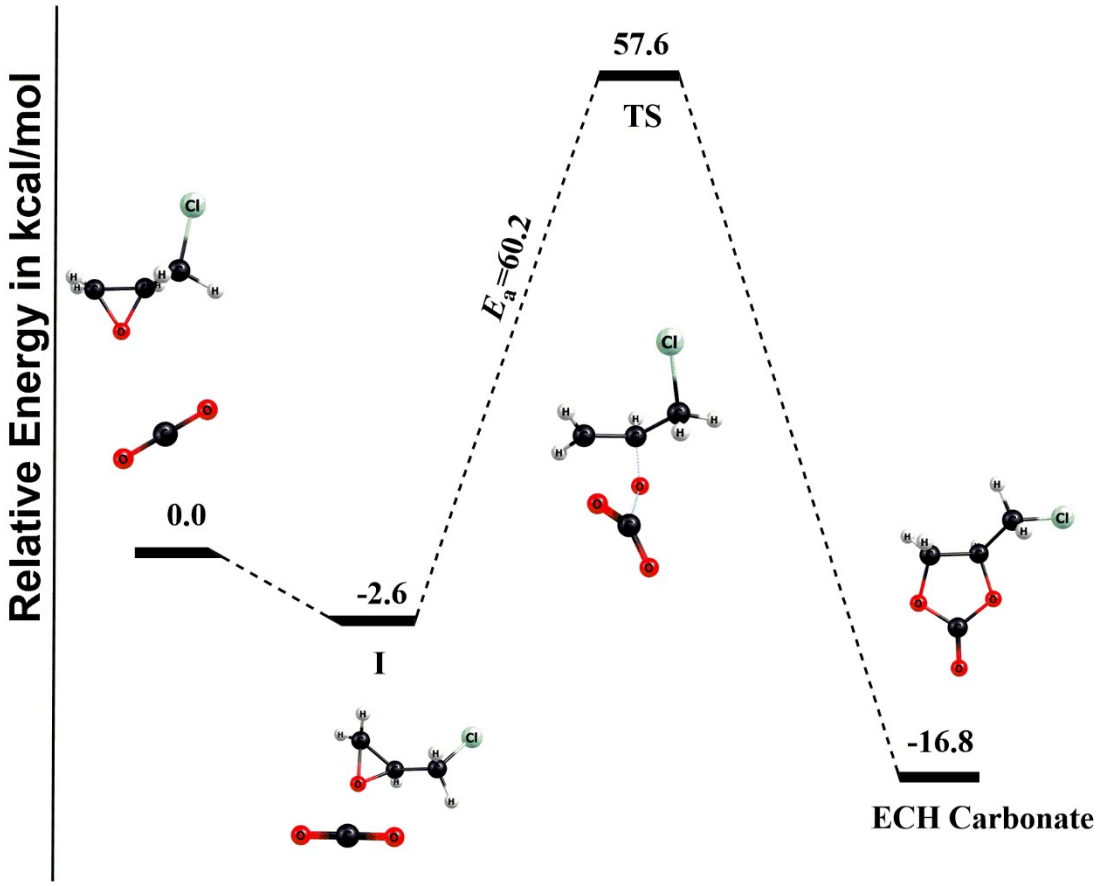

Fig. S13 Relative energy diagram of the un-catalyzed cycloaddition reaction of ECH and CO_2 to form chloropropene carbonate.

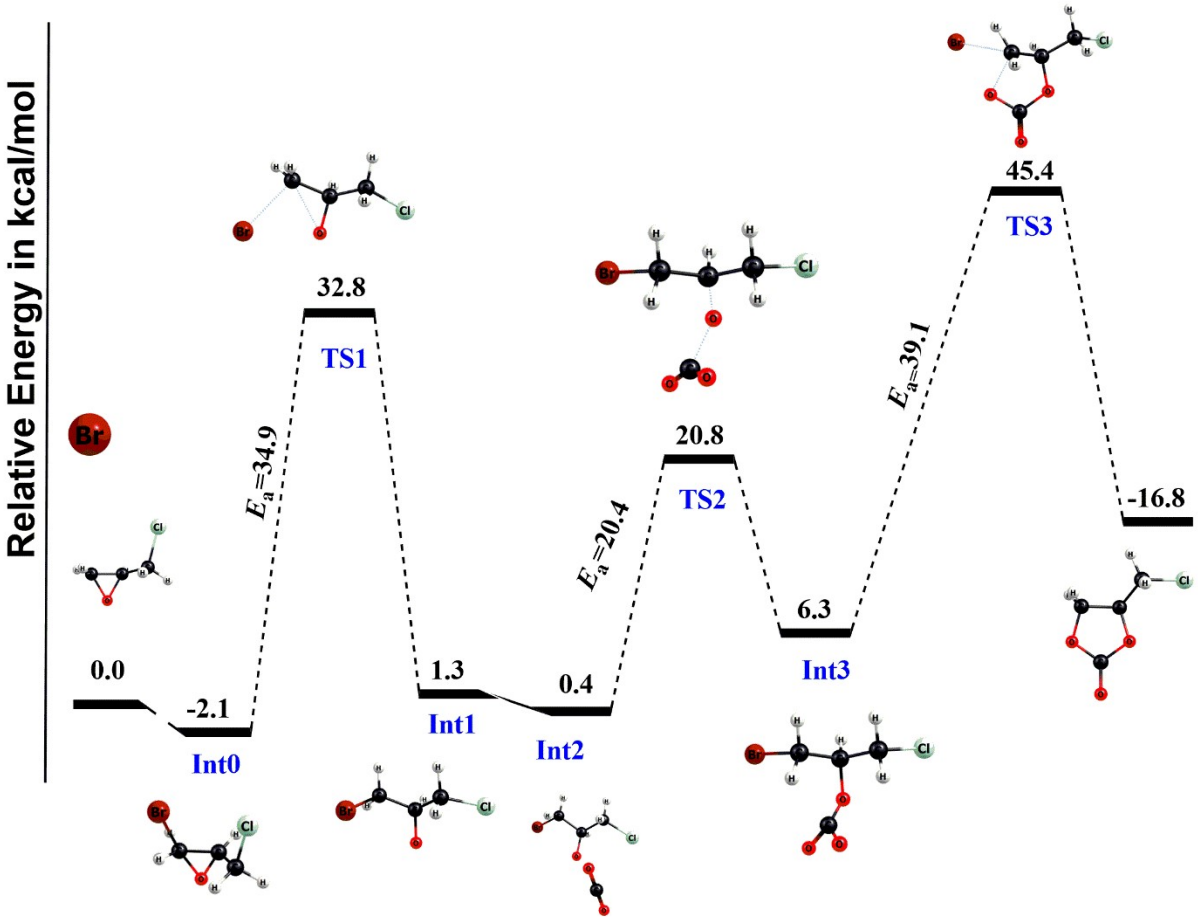

Fig. S14 Relative energy diagram of the -Br catalyzed cycloaddition reaction of ECH and CO_2 to form chloropropene carbonate.

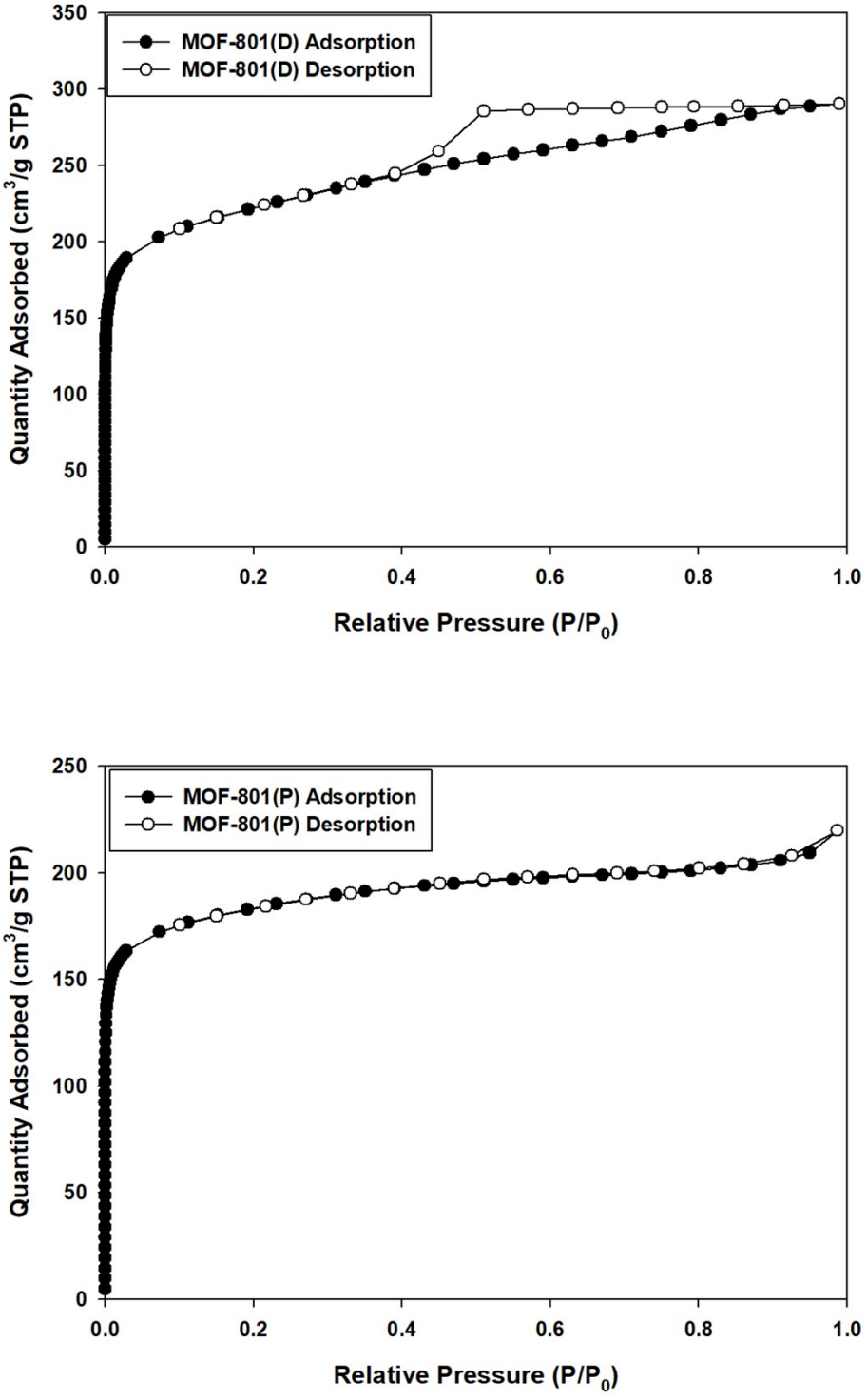

Fig. S15 N_2 adsorption isotherms of MOF-801(D) and MOF-801(P).